



Detection and tracking of chemical trails in bio-inspired sensory systems

Yangyang Huang^a, Jeannette Yen^b and Eva Kanso^a

^aAerospace and Mechanical Engineering Department, University of Southern California, Los Angeles, CA, USA; ^bSchool of Biology, Center for Biologically-Inspired Design, Georgia Institute of Technology, Atlanta, GA, USA

ABSTRACT

Many aquatic organisms exhibit remarkable abilities to detect and track chemical signals when foraging, mating and escaping. For example, the male copepod *T. longicornis* identifies the female in the open ocean by following its chemically flavoured trail. Here, we develop a mathematical framework in which a local sensory system is able to detect the local concentration field and adjust its orientation accordingly. We show that this system is able to detect and track chemical trails without knowledge of the trail's global or relative position. These findings could have implications on deciphering how organisms decode sensory information and on the development and deployment of bio-inspired sensory systems.

ARTICLE HISTORY

Received 29 March 2017
Accepted 3 April 2017

KEYWORDS

Chemical tracking;
bioinspired sensing;
underwater locomotion;
trail following

1. Introduction

The response to olfactory signals and pheromones plays an important role in a variety of biological behaviours (Dusenbery, 1992; Vickers, 2000; Zimmer & Butman, 2000) such as homing by the Pacific salmon (Hasler & Scholz, 2012), foraging by seabirds (Nevitt, 2000), lobsters (Basil & Atema, 1994; Devine & Atema, 1982) and blue crabs (Weissburg & Zimmer-Faust, 1994), and mate-seeking and foraging by zooplanktons and insects (Cardé (1996); Cardé & Mafra-Neto, 1997). These dissimilar organisms and behaviours share similar mechanisms of sensing and responding to chemical signals (Vickers, 2000). The underlying mechanisms could be applied or adapted to design artificial devices for source detection and tracking of chemicals in various environments, see examples in Grasso (2001), Pyk (2006), Nakatsuka, Kagawa, Ishida, and Toyama (2006), Dhariwal, Sukhatme, and Requicha (2004).

Evidence suggests that many organisms respond to concentration difference (= signal strength) and orient themselves to the desired direction, either moving towards or escaping from a source (Buck, 2000; Vickers, 2000; Johnson, Muhammad, Thompson, Choi, & Li, 2012). Copepods, a type of zooplankton

about 0.1 cm in length, exhibit similar abilities in responding to biological and physical gradients; see, e.g. Woodson, Webster, Weissburg, and Yen (2005) and references within. For example, copepods are known to aggregate at the boundaries of different water bodies in the ocean (Holliday, Pieper, Greenlaw, & Dawson, 1998). This aggregation is thought to be a result of the response to oceanic structures involving spatial gradients of flow velocities and densities (Woodson et al., 2005). Copepods adjust their swimming speed or turning frequencies with respect to these physical gradients in the water environment. Also, copepods sense biological gradients in mate-seeking (Doall, Colin, Strickler, & Yen, 1998). In careful laboratory experiments by Jeannette Yen that focus on the mating behaviour of the copepod *Temora longicornis*, a chemically scented trail that mimics the pheromone-laden trail of the female is introduced into a quiescent water tank. Male copepods are able to detect and successfully track the trail mimic to its source as shown in Figure 1.

In this work, we are loosely inspired by the copepod tracking ability of the female chemical trail. We develop an idealised, simple model where a moving chemical source generates a trail in an infinite two-dimensional space and a tracker is able to locally sense the chemical field and adjust its orientation accordingly to locate and track the trail. The organisation of this work is as follows. We first illustrate the chemical trail in Section 2 by reformulating the problem in the moving frame attached to the source. In Section 3, we study the conditions for successful tracking using a gradient-based tracking scheme. In the situation where the tracker is far away from the chemical trail such that the gradient information is not reliable, a random-walk phase is introduced to first detect the chemical signal before switching to the gradient-tracking method. The detection algorithm and results are described in Section 4. We conclude by summarising our findings and discussing their potential implications to understanding the behaviour of copepods in Section 5.

2. Problem description

Consider a chemical source moving at a constant velocity U from right to left in a fixed frame (X, Y) , shown in Figure 2(a). The concentration field is governed by the diffusion equation

$$\frac{\partial C}{\partial t} = K \frac{\partial^2 C}{\partial Y^2} + Q\delta(X + Ut)\delta(Y), \quad (1)$$

where Q is the rate of generation of the chemicals, K is the mass diffusivity of the chemicals and δ is the Dirac-delta function. In (1), we neglected diffusion in the X -direction. This assumption can be readily justified by calculating the Péclet number Pe , defined as the ratio of advective to diffusive transport rate. Large Pe ($Pe \gg 1$) implies that advection is dominant while for small Pe ($Pe \ll 1$) diffusion is dominant. In the X -direction, Péclet number is given by $Pe = LU/K$ where L

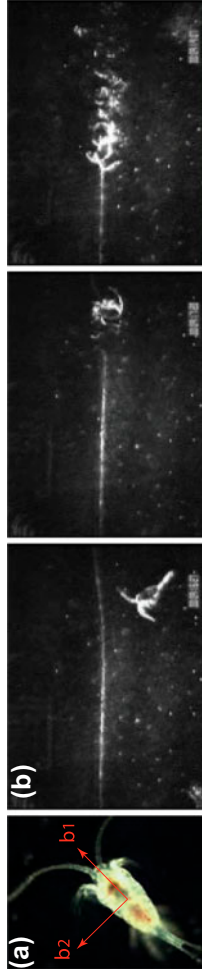


Figure 1. (a) Copepod *Temora longicornis* (~ 1 mm in length). Sensing of chemical signals is mediated by a distribution of small mechanoreceptive organs on its antennae. (b) Trail tracking by copepod: sequences showing the progression of the copepod *T. longicornis* while navigating a chemically flavoured laminar trail mimic. The copepod first follows the trail in the direction away from the source then corrects its heading direction and traces the trail in the direction of increasing chemical signal. The trail mimic is created by releasing fluid via syringe pump (0.01 mL/min) and small bore tubing (1 mm). Dextran, a large molecular weight, was added to increase refractive index of the trail, enabling us to see both the deformation of the signal and movement of the tracking copepod.

and U are the characteristic length and speed, which for a swimming copepod take the values $L = 0.1$ cm and $U = 1$ cm/s (Woodson, Webster, Weissburg, & Yen, 2007). The diffusivity coefficient involved in small biological organisms is of the order $K = 10^{-5}$ cm²/s (Lombard, Koski, & Kiørboe, 2013). Thus, $Pe \sim 10^4$ and diffusion is negligible in the X -direction.

It is convenient to rewrite Equation (1) in a reference frame (x, y) moving with the chemical source at a speed U , shown in Figure 2(b). The moving frame (x, y) is related to the fixed inertial frame (X, Y) via the transformation

$$x = X + Ut, \quad y = Y. \quad (2)$$

Therefore, $\frac{\partial C}{\partial t} = \frac{\partial C}{\partial t} + U \frac{\partial C}{\partial x}$ and Equation (1) becomes an advection–diffusion equation as

$$\frac{\partial C}{\partial t} + U \frac{\partial C}{\partial x} = K \frac{\partial^2 C}{\partial y^2} + Q\delta(x)\delta(y). \quad (3)$$

The steady-state solution of (3) is given by

$$C = \frac{Q/U}{\sqrt{4\pi(K/U)x}} \exp\left(-\frac{y^2}{4(K/U)x}\right). \quad (4)$$

A colour map of this concentration is shown in Figure 2 with pink indicating higher concentration values.

Next we study the tracking behaviour of a sensory system, or a chemical tracker, in response to these chemical signals. One natural example of chemical tracking is in the mating behaviour of copepods, where the female swims at a roughly constant speed along a straight path, while the male swims at faster speeds along a sinuous route until it detects the chemical trail left by the female and follows it Woodson et al. (2007). The female copepod has body length $L = 0.1$ cm and speed around $U = 1$ cm/s, leaving a trail of chemicals where $Q/U = 0.253$ μ g/cm³, or equivalently, the source rate is $Q = 0.253$ μ g/(cm² · s). We inherit these parameter values for our current study. In our simulation, we choose mass scale $m^* = 0.1$ μ g, velocity scale $U^* = U = 1$ cm/s and length scale $L^* = 10L = 1$ cm to non-dimensionalise the problem. This choice of length scale makes it more feasible to treat the tracker as a point particle.

3. Tracking of chemical trails

Consider a sensory system moving at a swimming speed V and let $(\mathbf{b}_1, \mathbf{b}_2)$ be an orthonormal frame attached to the sensory system such that \mathbf{b}_1 is aligned along the swimming direction; see Figure 2. Let θ denote the orientation of the \mathbf{b}_1 -axis measured from the \mathbf{e}_1 direction. The sensory system is able to sense the directional concentration gradients $s_1 = \nabla C \cdot \mathbf{b}_1$ and $s_2 = \nabla C \cdot \mathbf{b}_2$ and adjust its orientation, but not speed, based on the gradients it senses. In the moving frame (x, y) , we have

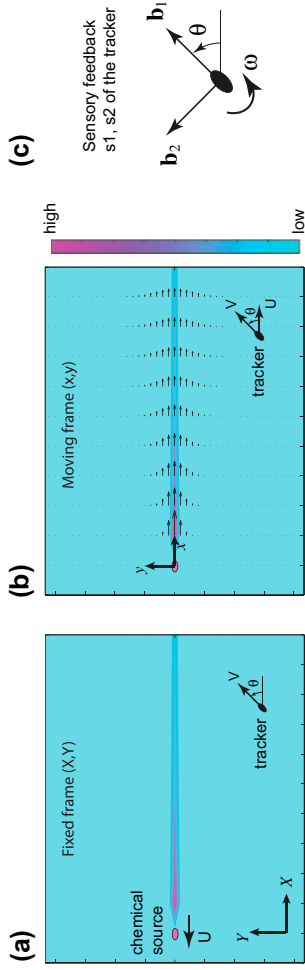


Figure 2. Chemical trail left behind a source moving at constant speed U to the left: (a) in fixed inertial frame (X, Y) and (b) in a frame (x, y) moving with the source. A sensory system (black ellipse) moving at a constant velocity V senses the chemical gradient in body-fixed frame b_1, b_2 and adjusts its orientation θ accordingly (c).

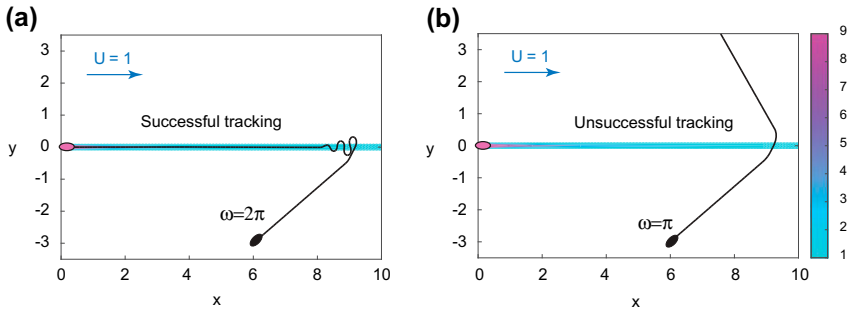


Figure 3. Successful and unsuccessful tracking for parameter values (a) $\omega = 2\pi, V = 2$ and (b) $\omega = \pi, V = 2$. Other parameters are set as $Q = 0.1, K = 10^{-5}$, and $\gamma = 0.01$. The initial location of the sensory system is $x(0) = 6, y(0) = -3$ and its initial orientation is $\theta(0) = \pi/3$. Colours represent the steady-state spatial distribution of the chemicals.

$$\dot{x} = U + V \cos \theta, \quad \dot{y} = V \sin \theta, \quad \dot{\theta} = F(s_1, s_2). \quad (5)$$

Here, we postulate a simple form of the function $F(s_1, s_2)$, namely,

$$F(s_1, s_2) = \omega \operatorname{sgn}(s_2) H(\gamma - s_1) \quad (6)$$

where ω is a constant rotation rate, $\operatorname{sgn}(\cdot)$ is the sign function and $H(\cdot)$ is the heaviside function. According to (6), if the concentration gradient $s_1 = \nabla C \cdot b_1$ in the b_1 -direction is larger than a threshold value γ , then $\dot{\theta} = 0$ and the sensor continues to move in the same direction. If s_1 is less than γ , one has $H(\gamma - s_1) = 1$ and $\dot{\theta} = \omega \operatorname{sgn}(s_2)$. In this case, the sensor turns with angular velocity ω into the direction of increasing concentration, indicated by the sign of $s_2 = \nabla C \cdot b_2$. Note that the tracking scheme depends on the sign of the signals instead of their exact values. Therefore, the results are not sensitive to the distance between the tracker and the chemical source, especially in the x -direction.

We simulate the trajectory of our sensory system by integrating Equation (5) in time using the adapted-time-step function ‘ode45’ in MATLAB. Basic parameter values are chosen as follows: source rate $Q = 0.1$, diffusivity $K = 10^{-5}$ and threshold $\gamma = 0.1$. The initial location of the sensory system is $x(0) = 6, y(0) = -3$. Figure 3 shows the trajectories for the same initial orientation $\theta(0) = \pi/3$ and swimming speed $V = 2$ but two sets of control parameters: (a) $\omega = 2\pi$ and (b) $\omega = \pi$. In (a), the tracker successfully follows the chemical trail while in (b) the tracker encounters the trail but fails to track it. This is because its angular velocity $\omega = \pi$ is not large enough for the sensory system to make a quick turn into the chemical trail. It is worth noting that the oscillatory trajectory in successful tracking is also found in the copepod experiments (Woodson et al., 2007).

We now examine the tracking behaviour of the sensory system with respect to the two control parameters: angular velocity ω and swimming speed V . Other parameter values and initial conditions remain the same as those in Figure 3.

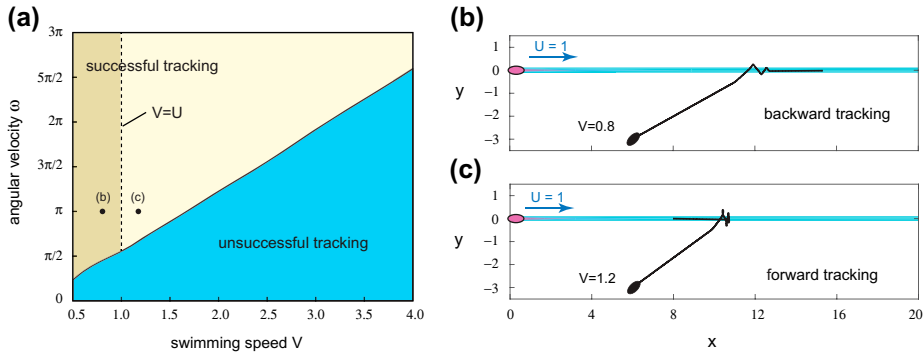


Figure 4. Tracking behaviour in the parameter space of swimming speed V and angular velocity ω . Other parameter values and initial conditions are the same as in Figure 3. (a) Parameter space (V, ω) of successful vs. unsuccessful tracking. (b) Successful backward tracking with swimming speed $V = 0.8$ less than the source speed $U = 1$. (c) Successful forward tracking with $V = 1.2 > U$.

We map the unsuccessful and successful tracking on the two-dimensional space (V, ω) in Figure 4(a). It shows that as the tracker swims faster, the required angular velocity ω for successful tracking also increases. The transition from unsuccessful to successful tracking displays a linear relationship between the angular velocity ω and the swimming speed V . Note that the chemical source has a speed $U = 1$. When the tracker's speed $V < U$, the tracking is in the opposite direction of the source location, which we denote as backward tracking. See the example in Figure 4(b) for $V = 0.8$ and $\omega = \pi$. Backward tracking of a chemical trail has already been observed in copepod experiments (Doall et al., 1998). When the tracker's speed is larger than that of the source, $V > U$, it tracks the chemical trail in the direction towards the location of the source, termed as forward tracking, shown in Figure 4(c) for $V = 1.2$ and $\omega = \pi$. The boundary separating these two types of successful tracking is illustrated as a dashed line at $V = U$. This boundary can be easily inferred from Equation (5) by setting $\theta = \pi$ where the tracker is heading into the direction of the source. To achieve forward tracking, the horizontal velocity \dot{x} must be in the negative x -direction; namely $\dot{x} = U - V < 0$. Both backward and forward tracking are successful in tracking the chemical trail but differ in their ability to locate the source.

The parameter space displayed in Figure 4(a) is specified for one initial orientation $\theta(0) = \pi/3$. We now explore the two-dimensional space (V, ω) in Figure 5(a)–(f) with respect to six different initial orientations: $\theta(0) = 0, \pi/3, \pi/2, 2\pi/3, 5\pi/6$ and π . When $\theta(0) = 0$ or π , the tracker moves in the positive or negative x -direction parallel to the chemical trail without ever turning or intercepting the trail. The sensory system fails to approach the chemical trail and therefore the tracking is unsuccessful irrespective of the values of V and ω . For initial conditions that intercept the trail, both unsuccessful and successful tracking can be achieved, as shown in Figure 5(b)–(e). Note that plot (b) is the same as the one in Figure 4. The boundary marking the transition from

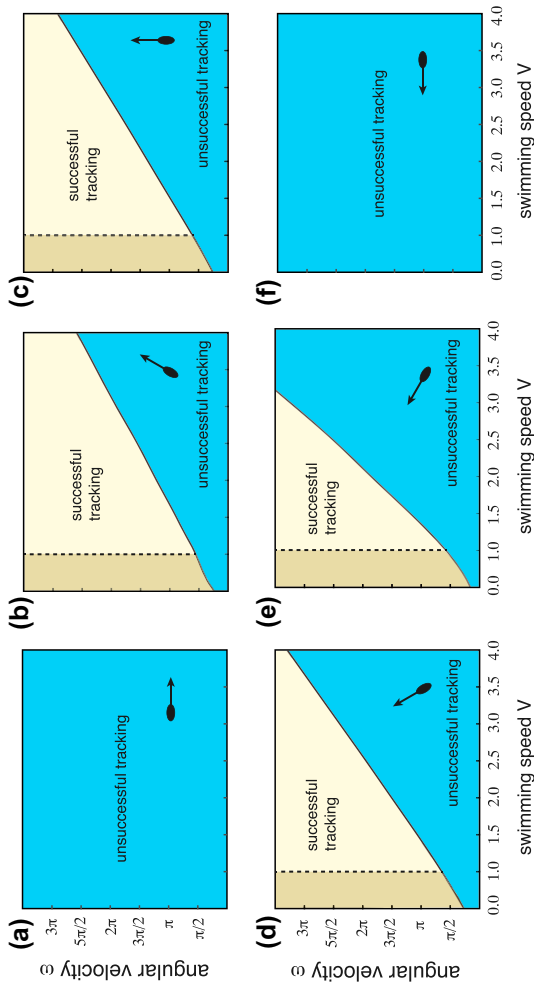


Figure 5. Parameter space of swimming speed V and angular velocity ω as a function of six different initial orientations $\theta(0) = 0, \pi/3, \pi/2, 2\pi/3, 5\pi/6$ and π , shown in (a)-(f) respectively. Dashed line is the interface between backward and forward tracking.

unsuccessful to successful tracking is given by a linear relationship between V and ω . The slope of the linear boundary gets steeper as $\theta(0)$ increases. In other words, as the angle between the tracker $\theta(0)$ and the trail becomes more obtuse, the tracker requires faster rotational motion for successful tracking. As $\theta(0) \rightarrow \pi$, the slope of the transition between unsuccessful and successful tracking tends to infinity. In Figure 5(b)–(e), the transition from backward to forward tracking is independent of $\theta(0)$ and bifurcates at $V = U$.

4. Detection of chemical trails

The gradient-based model for trail tracking is not feasible for the initial detection of the trail because at distances far away from the trail the gradient is too shallow to be accurately sensed. However, the local concentration itself can be sensed (Li, Farrell, Pang, & Arrieta, 2006). Therefore, we introduce a detection step to first find the strong chemical trail by comparing the local chemical concentration to a threshold value C_o . If the former is larger, then the chemical trail is detected and the tracker enters the tracking step using gradient information in (6). During the detection, the tracker executes a random walk that resembles the run-and-tumble behaviour of bacteria (Adler, 1966; Berg & Brown, 1972). That is to say, the tracker runs in the same orientation if the detected concentration is increasing otherwise it tumbles by randomly choosing a direction. An illustration of the detection algorithm is shown in Figure 6.

According to Figure 6, a tracker initially at (x_m, y_m) detects the local concentration as $C_m = C(x_m, y_m)$ and picks a random direction θ_m to start moving. After a given time $t_m = t_{m-1} + \Delta t$, where Δt is the time step and m is a positive integer, the tracker's position is given by $x_m = x_{m-1} + (U + V \cos(\theta_{m-1}))\Delta t$ and $y_m = y_{m-1} + V \sin(\theta_{m-1})\Delta t$. It senses a new concentration C_m at the new location (x_m, y_m) . If $C_m > C_o$, then the chemical trail is detected. Otherwise, the tracker executes the run-and-tumble behaviour by comparing the current concentration C_m to the previous one C_{m-1} . If $C_m > C_{m-1}$, the tracker runs without changing its orientation $\theta_m = \theta_{m-1}$. If $C_m < C_{m-1}$, then the tracker picks a random direction θ_m and follows that direction for N time steps. That is, $1/(N\Delta t)$ can be interpreted as the 'frequency' of random walk. At the time when the local concentration C_m achieves the threshold value C_o , the detection step ends and transitions to the gradient-tracking step. The total detection time is calculated as $t_d = m\Delta t$. Yet, if during a simulation, the time count m is greater than a given maximum value m_{\max} , then the detection is considered unsuccessful within the given amount of time $t_{\max} = m_{\max}\Delta t$. Note that if time is long enough, the tracker is guaranteed to detect the chemical trail in a two-dimensional plane (Borwein, Bailey, & Bailey, 2004; Spitzer, 2013).

The detection step is governed by four control parameters: the concentration threshold C_o , time step Δt , frequency N , and maximum detection time t_{\max} . Here, we choose $C_o = 10^{-5}$, $\Delta t = 0.01$, $N = 100$ and $t_{\max} = 20$ and study the

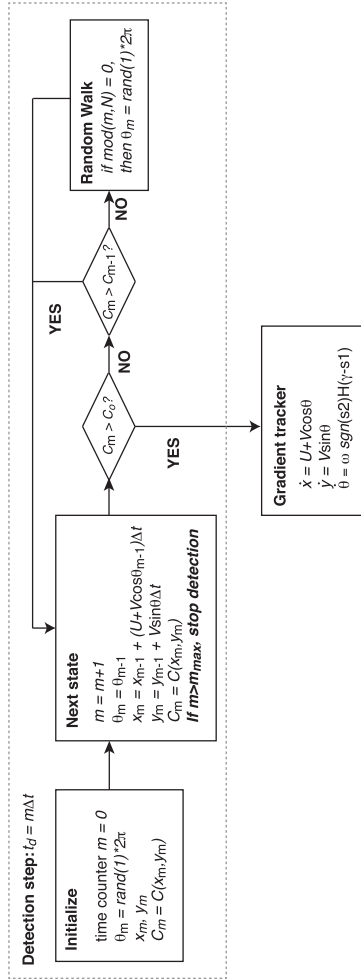


Figure 6. The run-and-tumble detection step of the chemical tracker. C_0 denotes the concentration threshold for the chemical trail. The tracker can detect the concentration C_m at its current location (x_m, y_m) and also remembers the previous concentration C_{m-1} . If $C_m < C_0$, the tracker runs and tumbles in the detection step. If $C_m > C_{m-1}$, it remains the current orientation θ_m . Otherwise, it executes a random walk with frequency N such that θ_m is randomly chosen in between 0 and 2π every N iterations of time step Δt . When $C_m > C_0$, the tracker stops the detection step and enters the tracking behaviour. If $m > m_{\text{max}}$, then the detection is unsuccessful.

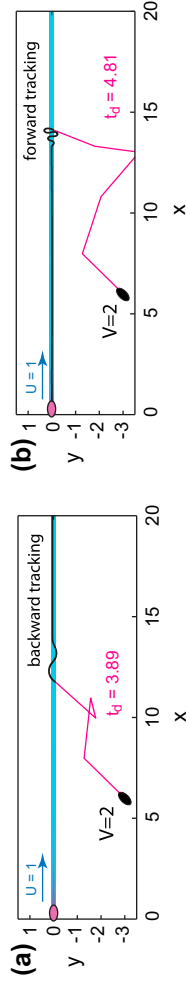


Figure 7. Two sample cases of random walk in the detection of chemical trail. Control parameters are set as follows: concentration threshold $C_o = 10^{-5}$, time step $\Delta t = 0.01$, random-walk frequency $N = 100$ and maximum detection time $t_{max} = 20$. The two trackers have the same initial conditions $x(0) = 6, y(0) = -3, \theta(0) = \pi/3$ and parameter values $\omega = 2\pi, V = 2$ but end up with different tracking behaviours: (a) backward tracking and (b) forward tracking.

effect of swimming speed V on the detection time t_d . In Figure 7, we show two sample trajectories starting at the same initial position $x(0) = 6, y(0) = -3$ and random initial orientation $\theta(0) = \pi/3$ for the same parameter values $\omega = 2\pi$ and $V = 2$. The two trajectories are distinct owing to the random nature of the search motion such that backward tracking occurs in (a) and forward tracking in (b). The detection time t_d , which we define as the total time it takes the sensory system to first detect the trail, is also not the same in the two simulations: $t_d = 3.89$ in (a) and $t_d = 4.81$ in (b). Note that the detection time t_d is independent of the angular velocity ω , which only participates in the tracking behaviour, but depends on the swimming speed V . In the copepod experiments (Doall et al., 1998), the dimensional detection time is up to 10 s.

Figure 8 depicts the histogram or distribution of detection time t_d of successful detections obtained from 1000 distinct simulations for the same initial locations shown in Figure 7 and three parameter values of $V = 1, 2, 3$. We fit the probability distributions to smooth exponential functions $P(t) = \lambda e^{-\lambda t}$, shown as red curves, such that the average detection time is $\langle t_d \rangle = 1/\lambda$. Note that the exponential fit is not perfect, but it is a closer analytical fit to the resulting distribution compared to a Poisson and normal distribution. The discrepancy between the analytical fit and the numerical data has minimal implications on the following results. As velocity increases, the decrease of the probability density function is steeper (larger λ) and the averaged detection time $\langle t_d \rangle$ decreases from 9.83 to 6.39 and 4.39. Therefore, larger swimming speed results in faster detection. In addition, out of the 1000 simulations we run, we keep track of the number of simulations which resulted in unsuccessful detection in $t_{\max} = 20$. We find that the ratio of unsuccessful detection to total number of simulations is 0.57, 0.3 and 0.26 for $V = 1, 2$ and 3, respectively. That is to say, faster swimming is also beneficial to more successful detections in a given amount of time.

We finally evaluate the average detection time $\langle t_d \rangle$ as a function of the tracker's initial location $x(0), y(0)$. The region of interest is chosen to be $[0.1, 10] \times [-5, -1]$ as shown in Figure 9. The colours indicate the values of the detection time at the corresponding initial locations, with red specifying longer detection time. We can see that $\langle t_d \rangle$ varies little in the x -direction especially in the range of $x(0) > 2$ meanwhile the average detection time decreases significantly when the horizontal distance between the tracker and the source is small $x(0) < 1$. The average detection time grows with increasing distances in the y -direction. These findings are consistent with the intuition that closer distance between the tracker and the source results in faster detection.

5. Conclusions

Odour tracking plays an important role in the behaviour of organisms at different scales and in different environments and could have significant implications on engineering and robotic applications. Inspired by the odour-tracking abilities

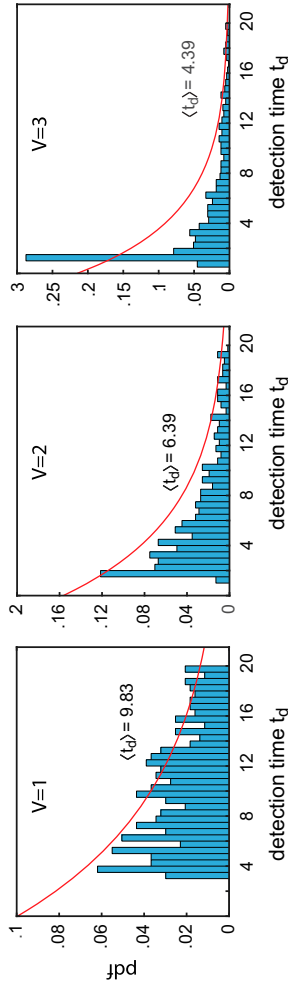


Figure 8. Probability distribution of detection time t_d with respect to different swimming speed V . The red curves are the fitted exponential probability density functions $P(t) = \lambda e^{-\lambda t}$ with $\lambda = 1/\langle t_d \rangle$, where $\langle t_d \rangle$ is the averaged detection time. For each value of V , 1000 distinct simulations are conducted to obtain the distribution of successful detections. The values of control parameters and also the initial locations of the tracker are the same as those in Figure 7.

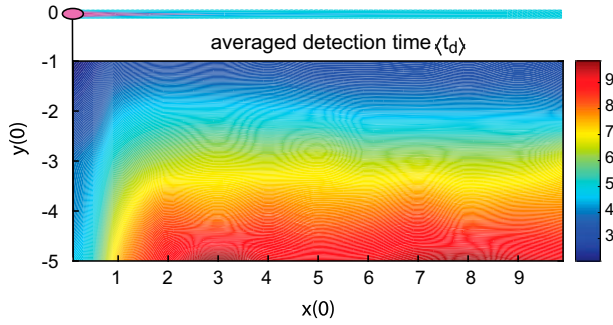


Figure 9. The averaged detection time $\langle t_d \rangle$ as a function of the tracker's initial location $x(0), y(0)$ in the region of $[0.1, 10] \times [-5, -1]$. Red colours represent longer detection time.

of male copepods in their mating behaviour, we simulated a sensory system that tracks and detects a two-dimensional chemical trail generated by a moving chemical source. The tracker can sense the local chemical gradients in its own body-fixed frame. The sensed gradients are used to control the orientation of the tracker such that it turns into the direction of increasing concentration. We identify the tracking behaviour as successful if the trajectory of the tracker ends up oscillating around or directly moving inside the chemical trail. Otherwise, the tracking is unsuccessful. Successful tracking consists of either backward or forward tracking. If the sensory system successfully tracks the trail but moves away from the source, then it is backward tracking. Backward tracking occurs when the speed of the tracker is less than that of the chemical source.

We then mapped the tracking behaviour onto the parameter space consisting of the speed V of the tracker normalised by the speed of the chemical source and the angular velocity ω of the tracker. The results show that higher V requires larger ω for successful tracking. The boundary marking the transition from unsuccessful to successful tracking follows a linear growth of ω as a function of increasing V . The parameter space (V, ω) changes with respect to the initial orientation $\theta(0)$ such that when the angle between the tracker and the trail becomes more obtuse (i.e. the angle between the velocity of the tracker and the velocity of the source is more shallow) the tracker requires both larger speed and angular velocity to succeed in tracking. That is to say, the tracker should speed up to successfully track the trail when the orientation of its velocity is close to that of the source.

A detection step is introduced when the chemical gradient is too weak to be accurately sensed by the tracker such as when the tracker is located far from the chemical trail. In this situation, the sensory system detects the chemical concentration first until the sensed local concentration is larger than a threshold value. The detection step is adapted from the run-and-tumble behaviour of bacteria such as *E. coli*, which runs when sensing a chemical signal or tumbles otherwise. In our implementation, the tracker continues in the same orientation if it senses an increasing concentration in that direction. If not, the tracker randomly picks

an orientation θ from 0 to 2π . If the detection takes longer than a given amount of time (the total simulation point), then the detection is unsuccessful. We illustrated the distribution of the detection time t_d obtained from 1000 distinct simulations and calculated the average detection time of successful ones. We found that the average detection time decreases with increasing speed V and the ratio of successful detection is higher when V is larger. Therefore, for a more successful detection, a fast speed V is preferred. We also showed that closer initial location to the source results in smaller detection time.

The two main results obtained from this study – the fact that both successful detection and successful forward tracking require the tracker to have larger swimming speed than the source and that the tracker's speed should be even larger when it swims nearly parallel to the source – are consistent with experimental observation of the copepod mating behaviour (Doall et al., 1998). Male copepods are known to swim faster than female copepods. While the reasons may be biological, this difference in speed between the male and female seems to have significant implications on successful detection and tracking of the female. Further, the detection time scale obtained here is consistent with experimental measurements of copepods (Doall et al., 1998). Male copepods are reported to detect the chemical trail in time intervals up to 10 s, which is similar to the average detection time reported in this study. Note that here one-dimensionless unit time scales to 1s.

A few remarks on the limitations of the model and future directions are in order. We considered a simple gradient-tracking model where the speed of the tracker and its turning rate are not affected by the intensity of the chemical signal. While this model was able to track the chemical trail, it would be interesting in future studies to compare this model to more complex models where the speed and turning rate change with the chemical signal. This study was restricted to two-dimensional tracking and detection but in many aquatic organisms, this behaviour is inherently three-dimensional. Also, we considered the chemical signal to diffuse in a quiescent environment. In many real-world applications, the environment is often characterised by unsteady and at time turbulent flows. Future work will extend the framework presented here to account for three-dimensional effects and the effect of flows and patchiness in the chemical signal (Weissburg & Zimmer-Faust, 1994; Kennedy & Marsh, 1974; Ishida et al., 1996; Kanzaki, 1996; Belanger & Willis, 1998). It is also interesting to couple the sensory and control framework presented here to more accurate models of the swimming mechanics; see Alben, Spears, Garth, Murphy, and Yen (2010) for an analysis of the details of such drag-based swimming and Catton, Webster, Brown, and Yen (2007) for an experimental study of the flow field generated by the swimming motion.

Disclosure statement

No potential conflict of interest was reported by the authors.

Funding

This work is partially supported by the Office of Naval Research through the [grant number ONR 14-001].

References

- Adler, J. (1966). Chemotaxis in bacteria. *Science*, 153, 708–716.
- Alben, S., Spears, K., Garth, S., Murphy, D., & Yen, J. (2010). Coordination of multiple appendages in drag-based swimming. *Journal of The Royal Society Interface*, 7, 1545–1557.
- Basil, J. & Atema, J. (1994). Lobster orientation in turbulent odor plumes: simultaneous measurement of tracking behavior and temporal odor patterns. *Biological Bulletin*, 187, 272–273.
- Belanger, J. H. & Willis, M. A. (1998). *Biologically-inspired search algorithms for locating unseen odor sources*. Proceedings of Intelligent Control (ISIC), 1998. Held jointly with IEEE International Symposium on Computational Intelligence in Robotics and Automation (CIRA), Intelligent Systems and Semiotics (ISAS) (pp. 265–270). Gaithersburg, MD: IEEE.
- Berg, H. C., & Brown, D. A. (1972). Chemotaxis in escherichia coli analysed by three-dimensional tracking. *Nature*, 239, 500–504.
- Borwein, J. M., Bailey, D. H., & Bailey, D. (2004). *Mathematics by experiment: Plausible reasoning in the 21st century*. Natick, MA: AK Peters Natick.
- Buck, L. B. (2000). The molecular architecture of odor and pheromone sensing in mammals. *Cell*, 100, 611–618.
- Cardé, R. T. (1996). Odour plumes and odour-mediated flight in insects. *Olfaction in mosquito-host interactions*, 200, 54–70.
- Cardé, R. T., & Mafrá-Neto, A. (1997). Mechanisms of flight of male moths to pheromone. *Insect pheromone research* (pp. 275–290). Springer.
- Catton, K. B., Webster, D. R., Brown, J., & Yen, J. (2007). Quantitative analysis of tethered and free-swimming copepodid flow fields. *Journal of Experimental Biology*, 210, 299–310.
- Devine, D. V. & Atema, J. (1982). Function of chemoreceptor organs in spatial orientation of the lobster, homarus americanus: differences and overlap. *The Biological Bulletin*, 163, 144–153.
- Dhariwal, A., Sukhatme, G. S. & Requicha, A. A. (2004). Bacterium-inspired robots for environmental monitoring. *Robotics and Automation, 2004*. Proceedings of IEEE International Conference on ICRA'04 (Vol. 2, pp. 1436–1443). IEEE.
- Doall, M. H., Colin, S. P., Strickler, J. R., & Yen, J. (1998). Locating a mate in 3d: the case of temora longicornis. *Philosophical Transactions of the Royal Society of London B: Biological Sciences*, 353, 681–689.
- Dusenbery, D. B. (1992). *Sensory ecology: How organisms acquire and respond to information*. New York, NY: WH Freeman.
- Grasso, F. W. (2001). Invertebrate-inspired sensory-motor systems and autonomous, olfactory-guided exploration. *The Biological Bulletin*, 200, 160–168.
- Hasler, A. D. & Scholz, A. T. (2012). *Olfactory imprinting and homing in salmon: Investigations into the mechanism of the imprinting process*, Vol. 14. Berlin: Springer Science & Business Media.
- Holliday, D., Pieper, R., Greenlaw, C., & Dawson, J. (1998). Acoustical sensing of small-scale vertical. *MicroCAT Sets the NEW Standard in Accurate Moored CT Instruments*, 11, 18.
- Ishida, H., Hayashi, K., Takakusaki, M., Nakamoto, T., Moriizumi, T., & Kanzaki, R. (1996). Odour-source localization system mimicking behaviour of silkworm moth. *Sensors and Actuators A: Physical*, 51, 225–230.

- Johnson, N. S., Muhammad, A., Thompson, H., Choi, J., & Li, W. (2012). Sea lamprey orient toward a source of a synthesized pheromone using odor-conditioned rheotaxis. *Behavioral Ecology and Sociobiology*, 66, 1557–1567.
- Kanzaki, R. (1996). Behavioral and neural basis of instinctive behavior in insects: Odor-source searching strategies without memory and learning. *Robotics and Autonomous Systems*, 18, 33–43.
- Kennedy, J. S. & Marsh, D. (1974). Pheromone-regulated anemotaxis in flying moths. *Science*, 184, 999–1001.
- Li, W., Farrell, J. A., Pang, S., & Arrieta, R. M. (2006). Moth-inspired chemical plume tracing on an autonomous underwater vehicle. *IEEE Transactions on Robotics*, 22, 292–307.
- Lombard, F., Koski, M., & Kjørboe, T. (2013). Copepods use chemical trails to find sinking marine snow aggregates. *Limnology and Oceanography*, 58, 185–192.
- Nakatsuka, T., Kagawa, Y., Ishida, H. & Toyama, S. (2006). Robotic system for localizing a chemical source underwater by mimicking crayfish behavior. *2006 5th IEEE Conference on Sensors* (pp. 416–419). Daegu, Korea: IEEE.
- Nevitt, G. A. (2000). Olfactory foraging by antarctic procellariiform seabirds: Life at high reynolds numbers. *The Biological Bulletin*, 198, 245–253.
- Pyk, P., Badia, S. B. i, Bernardet, U., Knüsel, P., Carlsson, M., Gu, J., ... Verschure, P. F. (2006). An artificial moth: Chemical source localization using a robot based neuronal model of moth optomotor anemotactic search. *Autonomous Robots*, 20, 197–213.
- Spitzer, F. (2013). *Principles of random walk*, Vol. 34. Berlin: Springer Science & Business Media.
- Vickers, N. J. (2000). Mechanisms of animal navigation in odor plumes. *The Biological Bulletin*, 198, 203–212.
- Weissburg, M. J. & Zimmer-Faust, R. K. (1994). Odor plumes and how blue crabs use them in finding prey. *Journal of Experimental Biology*, 197, 349–375.
- Woodson, C., Webster, D., Weissburg, M., & Yen, J. (2005). Response of copepods to physical gradients associated with structure in the ocean. *Limnology and Oceanography*, 50, 1552–1564.
- Woodson, C. B., Webster, D. R., Weissburg, M. J., & Yen, J. (2007). The prevalence and implications of copepod behavioral responses to oceanographic gradients and biological patchiness. *Integrative and Comparative biology*, 47, 831–846.
- Zimmer, R. K. & Butman, C. A. (2000). Chemical signaling processes in the marine environment. *The Biological Bulletin*, 198(2), 168–187.